

## Preliminary evaluation of nickel/cadmium cells for a totally implantable ventricular assist device

Zhi Xin Shu, Peter A. Aiken and Gregory K. MacLean\*

*Cardiovascular Devices Division, EVAD Program, University of Ottawa Heart Institute, Ottawa Civic Hospital, 40 Ruskin Avenue, Ottawa, Ont. K1Y 4M9 (Canada)*

William A. Adams

*Electrochemical Science and Technology Centre, University of Ottawa, 33 Mann Avenue, Ottawa, Ont. K1N 6N5 (Canada)*

(Received May 15, 1991; in revised form March 10, 1992)

### Abstract

A preliminary evaluation on the performance characteristics of three types of Ni/Cd cells was carried out in order to determine their potential usefulness in the internal (implantable) battery for the electrohydraulic ventricular assist device (EVAD) being developed at the University of Ottawa Heart Institute and University of Utah. The parameters studied at 37 °C were memory effect, discharge rate capability, self-discharge, surface temperature increase during charge and discharge and cycle life under the average power drain of the EVAD. Standard cells (designated 'S'), which were designed for room temperature use, suffered from a memory effect and had a low cycle life (114 cycles) and were, therefore, rejected for use in the EVAD. Two other types of cells (designated 'P' and 'H'), which were designed for higher temperature use, were comparable in their overall performance showing little or no memory effect and good cycle life (514 and 358 cycles, respectively). These latter two types of cells could be potential candidates for use in EVAD's internal battery.

### Introduction

One of the most common disorders causing suffering and premature death in our society is heart disease. The development of a mechanical device, namely a total artificial heart or a ventricular assist device, has been attempted by many researchers for more than two decades [1-3]. It has been proved clinically that these mechanical devices can be used to sustain the circulation during the recovery of the natural heart [4-7] or as a bridge to transplantation of a donor heart [8, 9]. To date, most commercially-available total artificial hearts and ventricular assist devices are pneumatically (air) powered. These devices are bulky and cumbersome and limit the mobility of the patient as they require the insertion of air hoses through the skin. Therefore, there is a great need to develop totally-implantable, or tether-free, artificial heart or ventricular assist device.

The Cardiovascular Devices Division of the University of Ottawa Heart Institute and the University of Utah are presently developing a totally-implantable electrohydraulic

---

\*Author to whom correspondence should be addressed.

ventricular assist device (EVAD). The source of energy for the EVAD is provided from either an external and an internal power source. The external electric power can be provided from either a.c. mains or from a portable battery. The external energy is transferred to the implanted device via an inductively-coupled transcutaneous energy transfer (TET) system. The external d.c. power is converted to radio frequency and transferred across the skin where it is then converted back to d.c. power. Internal power is provided by a battery of appropriate capacity and of suitable size and weight for implantation. The internal battery provides an extra feature for the EVAD recipients which pneumatic devices do not. Patients are able to be completely free (i.e. to take a shower, etc.) from the external power source of a specified period of time. In addition, the internal battery provides an extra operating margin of safety in case of unexpected external power failure. Figure 1 shows a schematic of the internal and external power sources in relation to other components of the EVAD, which have been described in more detail elsewhere [10]. Power source options for these devices have been reviewed recently by several authors [11–14].

Sealed nickel/cadmium (Ni/Cd) cells have been widely used in industrial and consumer applications because they provide high-rate capability, long cycle life and relatively high reliability. These characteristics make the Ni/Cd cell an attractive candidate for the internal power source of the ventricular assist device. However, for most consumer applications, Ni/Cd cells are utilized at room temperature where they provide their peak performance. In the EVAD application, Ni/Cd cells could potentially be used as its internal power source and will need to operate effectively at body temperature (37 °C). Nickel/cadmium cells have been successfully used to power cardiac

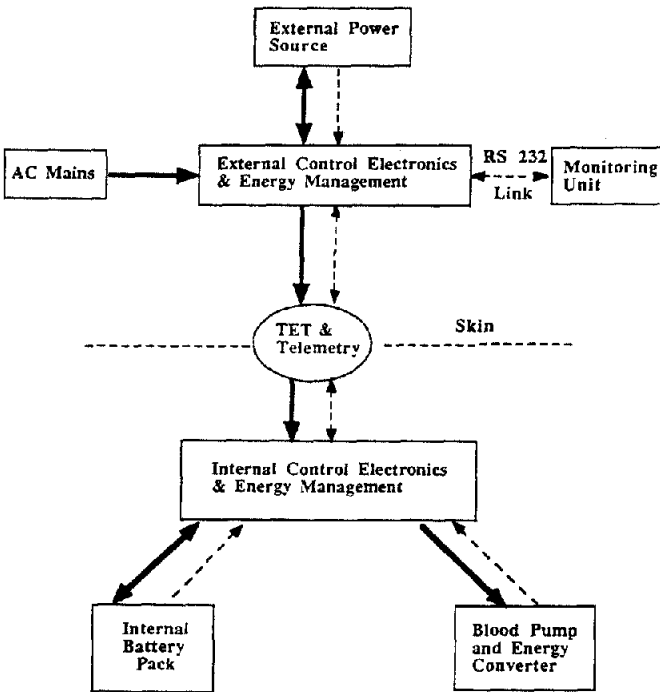


Fig. 1. A schematic depicting the EVAD components: (→) energy transfer; (---) data transfer.

pacemakers [15–17] by Pacesetter System Inc. The cells were operated at a very mild depth-of-discharge and low discharge current. Unfortunately, we have been unable to find any literature references dealing with the investigation of Ni/Cd cell performance at moderate or high discharge rates at 37 °C.

In this paper, a preliminary study of the performance of Ni/Cd cells at 37 °C was carried out in terms of their discharge rate capability, self-discharge phenomenon, memory effect, cell surface temperature change during charge and discharge and cycle life under EVAD conditions and average discharge load (0.875 A). This average discharge load was determined from the power requirements (10.5 W) of EVAD's energy converter and the nominal operating voltage (12 V) of the battery pack. The EVAD will require an internal battery that has a service life of one year and a volume and weight of less than 120 ml and 250 g, respectively. These volume and weight requirements restrict the size of the cells used for this application to the 'AA' size or smaller. Some studies were also carried out at room temperature for comparison. Three types of Ni/Cd cells were studied and their performances were compared. The feasibility of using Ni/Cd cells for implantation in the EVAD application is discussed in terms of these preliminary results.

## Experimental

Three types of commercially-available Ni/Cd cells were studied and were denoted as 'S', 'P' and 'H' cells. The 'S' and 'H' cells were 1.2 A h 'Cs' size cells, whereas 'P' cells were 2.0 A h 'C' size cells. The 'S' type cells were of a standard consumer grade and were rated best for room temperature applications, while the 'P' and 'H' type cells were designed for use in higher temperature (i.e. > 25 °C) applications.

The cells were cycled using an automatic battery cycler (Techware Systems, Model ABC). The battery cycler was controlled by a Stride computer (Model-430, Stride Micro) and supported by battery cycling software developed by Techware Systems. Some of the tests on the above cell sizes were performed at higher currents than required for the EVAD in order to approximate the current densities of 'AA' size cells required for the EVAD's internal battery due to size and weight constraints. For conversion purposes in our study, we have assumed that a 'AA' size cell has a capacity of 0.6 A h. The larger size cells were used because of the nature of the in-kind support of the EVAD project or availability of cells at the time of purchase. Unless otherwise stated, all experiments were carried out at 37 °C in a temperature-controlled ( $\pm 0.2$  °C) environmental chamber (Tenney Engineering, Inc., Model TH-Jr.).

Cell capacity matching was carried out by cycling 'S' type cells using a relay-controlled battery cycler, that was developed in-house, and which was used in conjunction with a Helios Data Acquisition System (Fluke Electronics Inc., Model #2289A) and Labtech Notebook software (Laboratory Technologies Corp., Ver. 5.01). These cells were cycled five times at room temperature using a 120 mA charge for 18 h followed by a 240 mA discharge to 1.0 V. Ten capacity-matched (i.e.  $\pm 5\%$  of their mean value of 1.35 A h) 'S' type cells were selected and then assembled into a series-connected battery, which was utilized in the 'capacity fade' study below.

### *Memory effect*

One cell of each type was used in this study. The cells were charged at a C/10 rate (0.12 A for 'Cs' size cells and 0.2 A for 'C' size cells) for a period of ten days, and were then discharged to 1.0 V at a C/5 rate for 'S' and 'P' type cells and a

3/4 C rate for 'H' type cells. A reconditioning cycle was applied to the cell, when a memory effect was evident from the first discharge step after overcharging. The reconditioning cycle consisted of several cycles of charging at a C/10 rate for a period of 16 h followed by deep discharge to 0.6 and 0.0 V at a C/5 rate.

#### *Surface temperature*

One cell of each type was used in this study. The cells were taped flat to a polystyrene foam holder with a thermocouple wire (T type, Omega) placed between the surface of each cell and the holder. An additional thermocouple wire was taped to the side of the holder and measured the ambient temperature within the environmental chamber. The upper surface of the cells were exposed to circulated and thermostated air at 37 °C. The temperatures from the thermocouples were measured and recorded during cycling of each cell using a data acquisition system. Their charge and discharge conditions were C/10 and 1.5 C rates respectively. This discharge rate was used to approximate what the 'AA' size cells would experience under the EVAD conditions.

#### *Discharge rate*

Four 'H', five 'P' and three 'S' type cells were used in this study. These quantities of cells were used in order to obtain a similar discharge rate capability, up to 2.0 C rate, between two cells of each type. The cells were charged at a C/10 rate and were discharged at different discharge rates to a voltage of 1.0 V. The discharge currents varied from 0.24 to 3.0 A (C/5 to 2.5 C) for 'H' and 'S' type cells and from 0.4 to 5.0 A (C/5 to 2.5 C) for 'P' type cells, respectively. Several cycles, using a 'standard' discharge current, were inserted in between those cycles in which different discharge currents were used. The cell capacities of these 'standard' cycles were used to determine the normal reduction in cell capacity due to cycling or 'natural capacity fade'. The capacity decrease resulting from the discharge rate alone was then calculated using a different method. The 'standard' currents used were 0.4 A, 0.24 A and 0.875 A for the 'P', 'H' and 'S' type cells, respectively.

#### *Self-discharge*

Two cells of each type were used in this study. The cells were charged at a C/10 rate for 15 to 16 h and discharged at a constant current to 1.0 V. The 'H' type cells were discharged at 0.875 and 1.8 A, the 'P' type cells were discharged at 1.5 A and the 'S' type cells were discharged at 0.875 A. A series of open-circuit periods ranging from 1 to 24 h were imposed in between the charge and discharge steps. In addition, a series of cycles that contained no open-circuit period were imposed in between those cycles which contained an open-circuit period. The cycles without an open-circuit period gave only the 'natural capacity fade' component of the capacity loss. This information could then be used, as in the discharge rate study, to correct for the 'natural capacity fade' due to cycling.

#### *Capacity fade*

'H' and 'P' type cells, on each, and a 12 V battery pack, containing capacity matched 'S' type cells, were used in this study. Both the cells and battery pack were charged at a C/10 rate (typically 16 to 23 h). The discharge conditions were different for each experiment. The 'H' and 'P' type cells were discharged at 1.8 A (1.5 C) and at 2.7 A (1.35 C) respectively, whereas the 'S' type battery was discharged at 1.75 A (1.46 C). The discharge end-point condition was set to either 80% depth-of-discharge or 1.0 V for the cells and 10.0 V for the battery pack, whichever came first. The

measurement from the 'S' type battery represents the average behaviour of ten cells. The voltages of each cell within the battery were also monitored periodically using a data acquisition system.

## Results and discussion

### *Memory effect*

Memory effect may occur when a Ni/Cd cell is overcharged for a prolonged period of time or is under a repetitive cycling regime to a particular depth-of-discharge less than 100%. The memory effect causes a potential step or decrease of approximately 100 mV per cell near the end-of-discharge. The memory effect was first noticed in satellite batteries and the mechanism that causes this decrease in voltage is still controversial. The original explanation of the memory effect was the formation of large cadmium hydroxide crystals at the cadmium electrode [18, 19]. The voltage drop observed was assumed to be the result of increased polarization associated with discharging the large particles at a higher-current density. More recently, Barnard *et al.* [20] studied the memory effect using electrochemical synthesis of active materials and X-ray diffraction techniques. They suggested that formation of an intermetallic compound or alloy  $\text{Ni}_{15}\text{Cd}_{21}$  at the cadmium anode was responsible for the memory effect. The voltage step was explained by the fact that the  $\text{Ni}_{15}\text{Cd}_{21}$  alloy had an electrochemical potential approximately 100 mV lower than that of cadmium. They also found that the memory effect became more severe at higher temperatures and under continuous overcharge conditions.

The direct impact of the memory effect on the performance of the EVAD is that the operating time of the implanted battery may be reduced, as the device can only operate within the range of 10–20 V. If the memory effect occurred in every cell of the battery pack, the operating time would be reduced by as much as 50%. Under normal circumstances, if a battery suffers from the memory effect, it may be reconditioned by several cycles of deep discharge. However, in the EVAD application, uncontrolled reconditioning of the battery is unacceptable as this would result in the patient having no emergency back-up power following the deep discharge. The EVAD application presents a problem in that the internal battery may be subjected to both prolonged overcharging and to repetitive discharging to a certain depth-of-discharge, both of which create a memory effect in Ni/Cd cells. Our design goal is to optimize battery performance without affecting the overall operation and reliability of the device. Therefore, the selection of batteries that do not develop a memory effect is highly desirable. In the case where a memory effect does occur, a strategy of battery management to minimize or remove the memory effect becomes an important design criterion.

Figure 2 shows the first discharge curves to a voltage of 1.0 V after 10 days of overcharge at a  $C/10$  rate for the three types of cells. The horizontal axis is normalized, as the discharge current for the three cell types are different. Both 'P' and 'H' type cells showed no indication of the memory effect. On the other hand, the 'S' type cell showed a potential step with a voltage depression of about 110 mV. This voltage decrease was removed, with some difficulty, by subjecting the cell to several reconditioning cycles. The potential step became less pronounced after three discharges to 0.6 V, but it was not completely removed until the cell was subjected to three more discharges to 0.0 V.

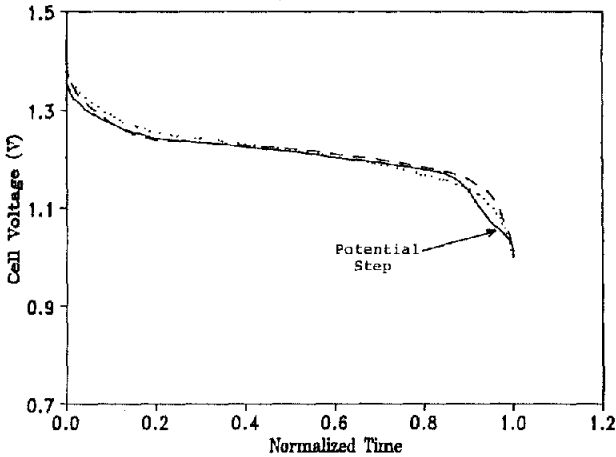


Fig. 2. Voltage-time curves of the first discharge after overcharging at a  $C/10$  rate for 10 days: (.....) 'P' type cell; (----) 'H' type cell; (—) 'S' type cell.

### Surface temperature

During charge and discharge of a Ni/Cd cell, its surface temperature changes. During initial charging, the temperature decreases as the charging is an endothermic process [21, 22]. As the charging proceeds, oxygen is generated. The endothermic charging and exothermic oxygen recombination processes offset each other and result in no net temperature increase. When a cell is almost fully charged, the oxygen recombination process becomes predominant and a temperature increase is detected. At a  $C/10$  charge rate, the oxygen generation and recombination processes reach a steady state and the final temperature increase remains relatively constant. During discharge, the chemical process is exothermic. The cell's internal resistance is another source of temperature increase.

Previous investigations have shown that body tissue can withstand long-term exposure to temperatures no greater than  $42.6\text{ }^{\circ}\text{C}$  [23, 24]. In our experiment, the measurements were taken from possibly the worst heat-transfer condition that would be encountered in the body. The cell was in contact with an insulator (i.e. polystyrene foam) on one side and air thermostated to  $37\text{ }^{\circ}\text{C}$  on the other. The mode of heat removal was primarily from the convection of air above the cell. This compares with a possible implantation site where blood circulation is expected to carry the heat away from the titanium encased battery pack through conduction.

The surface temperatures for the three types of cells were recorded, as a function of time, while being cycled at the average EVAD charge and discharge currents. The maximum surface temperature increases are given in Table 1 and a typical temperature-time profile is shown for the 'H' type cell in Fig. 3. Clearly, the temperature measurements from this experiment do not give what the body would experience when the battery is implanted, but rather, they provide an estimate of the possible temperature increase. Since the heat-transfer environment of this experiment is expected to be worse than in the implantation site, the temperature measurements from this experiment indicate a possible worst case scenario.

All three types of cells showed relatively similar surface temperature increases of 2 to  $4\text{ }^{\circ}\text{C}$  above ambient or body temperature during their charge, which is below the maximum allowable temperature increase of  $5.6\text{ }^{\circ}\text{C}$ . The surface temperature

TABLE 1

Maximum surface temperature increases above 37 °C during cycling of the three types of Ni/Cd cells

Cell types	Cycle step	Current (A)	Maximum $\Delta$ temperature (°C cell bottom)
'S'	charge	0.12 (C/10)	3.6
	discharge	1.80 (1.5 C)	8.3
'H'	charge	0.12 (C/10)	2.5
	discharge	1.80 (1.5 C)	4.8
'P'	charge	0.20 (C/10)	3.6
	discharge	2.70 (1.35 C)	8.5

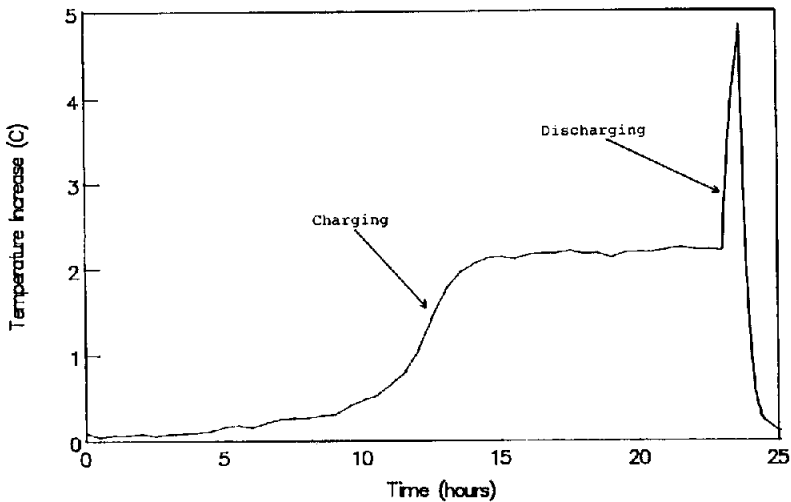


Fig. 3. Surface temperature profile for a 'H' type Ni/Cd cell during charge and discharge at 37 °C.

increases during the discharge of the 'S' and 'P' type cells was about 8 to 9 °C above ambient temperature (i.e. beyond the safe threshold of 5.6 °C), while that for the 'H' type cell was less than 5 °C. However, because the environment in this experiment is different from that for an implanted battery, we cannot conclude that the observed temperature increases during discharge are definitely unacceptable. Nevertheless, these temperature increases show the importance of choosing not only a good battery implantation site, but also battery cells which have low internal resistances.

#### Discharge rate

During daily operation of the EVAD, the power demand varies depending on a particular physical activity of the patient. For example, the energy requirement will be relatively low if the EVAD-patient is sleeping, as the heart rate will be low. Alternatively, the energy requirement will be high if the patient is exercising. Other abnormal health conditions, such as a fever, may also introduce temporary high-power

demands. The discharge-rate study provides information on: (i) whether or not a cell can provide sufficient capacity under a particular discharge current; (ii) to determine its operating time at these load conditions; (iii) to observe the cell's discharge voltage-time profile under various load conditions.

In our study, a cell is considered to have 'acceptable' discharge capability if it is able to deliver more than 50% of the manufacturer's rated capacity at a particular discharge current. Results on four 'H' type, five 'P' type and three 'S' type cells showed: (i) two 'H' type cells were unable to deliver usable capacity above a 1.25 C discharge rate, while two other cells gave 'acceptable' capacities at discharge currents above a 2.5 C rate; (ii) two 'P' type cells did not deliver 'acceptable' capacity at the 1.0 C discharge rate, one other cell could not supply 'acceptable' capacity above a 1.5 C rate and the remaining two 'P' type cells delivered 'acceptable' capacities up to 2.0 C and 2.5 C rates, respectively; (iii) all three 'S' type cells provided 'acceptable' capacities at the 1.5 C discharge rate and two of which provided 'acceptable' capacity at the 2.5 C rate. The reason for some of the cells having low discharge capability is probably due to their high internal resistances. We speculate that the performance variations may come from differences in the manufacturing process. Therefore, stringent in-house quality assurance and control procedures are required to ensure that only high quality cells are used.

As mentioned in the experimental section, the capacity of a cell is reduced slightly during each consecutive cycle. To a first approximation, the reduction in measured capacity from the experiment consists of two fractions: capacity reduction due to the high discharge current and the natural capacity fade due to cycling. Figure 4 shows the normalized corrected capacity, as a function of discharge rate, for those cells which exhibited good discharge capability. These capacities have been corrected for natural cycling capacity fade and have been normalized in order to better compare the three types of cells. All three cells show an approximately linear decrease in capacity with increasing discharge rate. If 'AA' size cells were used, they would experience a 1.5 C discharge rate. It was found that only a fraction of the rated capacity was available at this discharge rate. The observed capacity was 62, 74 and 79% of the rated capacity for the 'P', 'S' and 'H' type cells, respectively.

Cell voltages are typically depressed with increasing discharge currents. The midpoint voltage (MPV) is defined as the cell voltage at one half of the cell's discharge capacity and can be determined from the cell's discharge voltage-time profile. Figure 5 shows plots of the MPV, as a function of discharge rate, for the three types of cells studied. An approximate linear decrease in MPV with increasing discharge rate was observed for all three types of cells. This linear feature of the graph reflects the fact that ohmic polarization within the cells is the dominate factor resulting in the observed 'IR' or voltage drop in the cell's voltage. The effect of the discharge rates on the discharge voltages is least for the 'H' type cell and are similar for the 'S' and 'P' type cells. If Ohm's law is assumed to apply, the slopes of the graph will represent the effective internal d.c. resistance of cells. Therefore, from the slope of the lines in Fig. 5, the observed internal cell resistances at their 50% capacity points are calculated to be 20, 50 and 50 m $\Omega$  for the 'H', 'S' and 'P' type cells, respectively. The observed midpoint voltages for the 'H', 'S' and 'P' type cells at the 1.5 C discharge rate are 1.21, 1.15 and 1.15 V, respectively. Therefore, ten cells can be used in the internal battery and a battery voltage of 12 V can be employed when designing the peak operating efficiency of the motor.

The effective or operational energy density and specific energy of a cell or battery are also important parameters in the selection of an implanted power source. It is



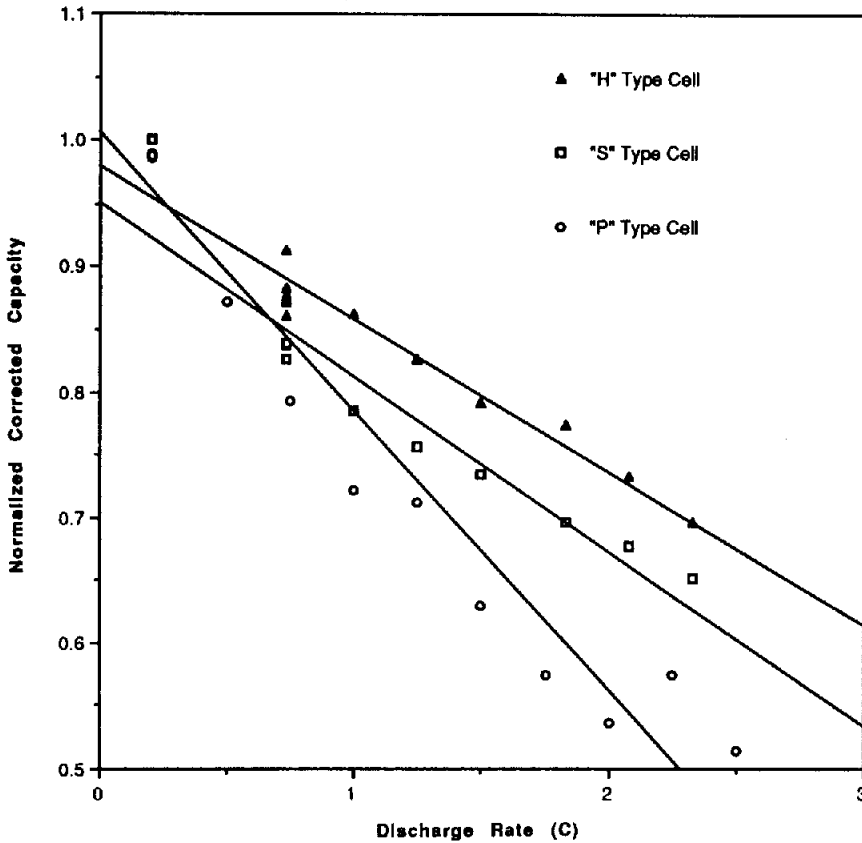


Fig. 4. Normalized corrected capacity as a function of discharge rate for the three types of Ni/Cd cells at 37 °C.

desirable that these parameters be maximized due to the constraints of size and weight on any implanted device. The effective energy density and specific energy for the cells can be calculated for the average EVAD load conditions by using their size and weight, as well as their midpoint voltages and cell capacities obtained at the 1.5 C discharge rate. This calculation yields effective energy densities of 78, 78 and 68 W h/l and similar effective specific energies of 24, 25 and 24 W h/kg for the 'H', 'S' and 'P' type cells, respectively.

#### *Self-discharge*

Self-discharge of a charged cell is defined as the loss in capacity during open-circuit storage. The cause of the self-discharge phenomenon in Ni/Cd cells is the result of two electrochemical mechanisms. Firstly, nickel oxyhydroxide, NiO(OH), oxidizes water at electrode sites having low oxygen overvoltages. The oxygen, so generated, diffuses to the cadmium electrode and is reduced [25–27]. The net result is a loss of charge at both electrodes. Secondly, parasitic side reactions caused by impurities introduced during the production process occur. One example of such an impurity is nitrate ions which form a nitrate shuttle between the two electrodes [28]. Most cells have accelerated self-discharge rates at high temperatures.

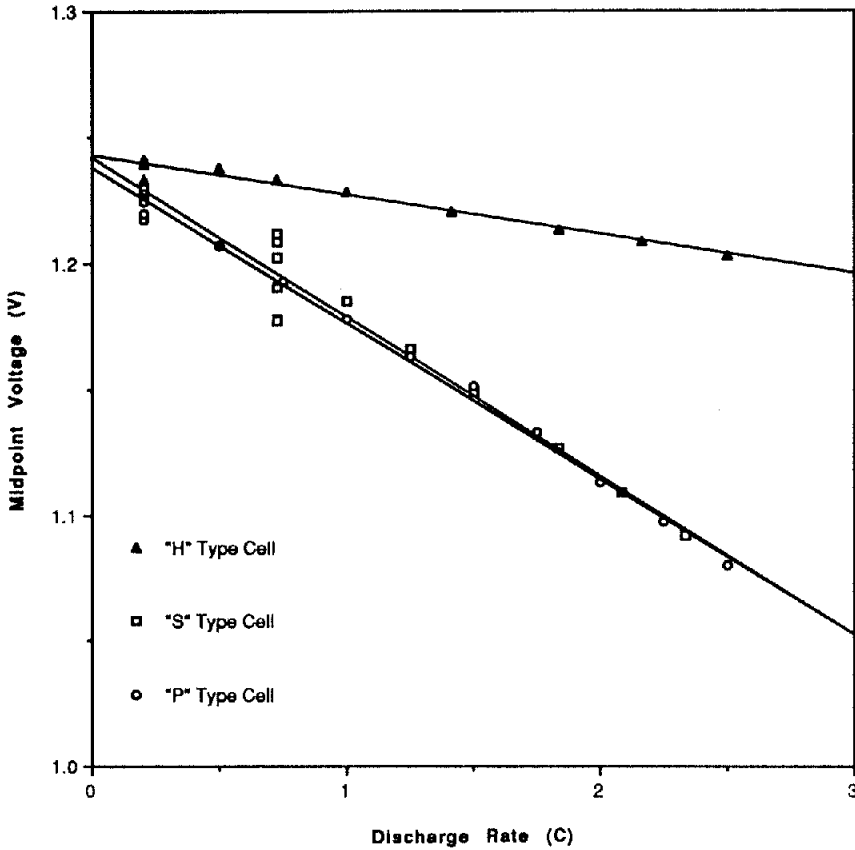


Fig. 5. Midpoint voltage as a function of discharge rate for the three types of Ni/Cd cells at 37 °C.

In the EVAD design, the internal battery only operates for about 0.5 h/day. During the remaining 23.5 h, the internal battery is either being charged or is in an open-circuit standby state after being fully charged. Therefore, it is important to study the self-discharge phenomenon of the internal battery, as it is required to deliver a specified operating time after being charged. The objective of this study is to determine the self-discharge behaviour of each cell type at 37 °C for open-circuit periods of up to 24 h. If the self-discharge is excessive, an appropriate charging regime must be introduced to compensate for the capacity loss.

As in the discharge rate study, the capacity change observed from the self-discharge study may be assumed to come from two effects: (i) the normal capacity fade during cycling; (ii) the capacity fade due to self-discharge. Figure 6 shows the normalized corrected capacity, as a function of the open-circuit period, for the three types of cells. These capacities have been corrected for natural cycling capacity fade and have been normalized in order to better compare the three types of cells. The asymptotic trend in the reduction of capacity with increased open-circuit period appears to be similar for all three types of cells. The 'P' type cells showed a reduction in capacity

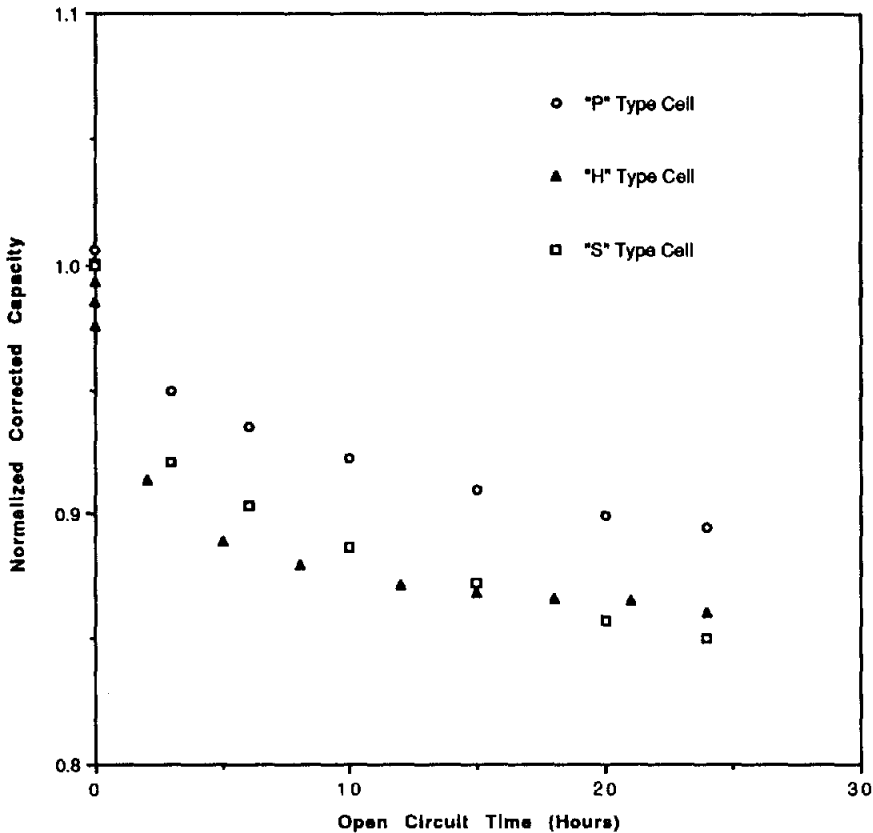


Fig. 6. Normalized corrected capacity as a function of open-circuit time for the three types of Ni/Cd cells at 37 °C.

of about 10% in 24 h, while the 'H' and 'S' type cells showed a slightly higher reduction in capacity of about 13 and 15% in 24 h, respectively.

#### Capacity fade

All cells lose capacity during cycling. The main mechanism of their capacity fade is the 'wear-out' effect (except premature failure). The 'wear-out' effect comes from deterioration of electrolyte, separators and sealing materials. Potassium hydroxide, in the presence of oxygen, reacts with the organic components, such as separators and sealing materials, to form carbonates. Another source of carbonate formation is from absorption of carbon dioxide from air during the manufacturing process. The presence of carbonates decreases the conductivity of electrolyte and, in turn, leads to a lower discharge voltage and capacity for a given termination voltage and discharge load [29]. The high-rate charge and discharge capabilities and effectiveness of the oxygen recombination are also reduced. Degradation of the separator materials may lead to an internal short circuit or a high rate of self-discharge. Both of which would result in lower cell capacity. Deterioration of the sealing materials will eventually lead to venting. However, this would not normally occur as other modes of failure often occur

beforehand. Many other factors also affect capacity loss, such as cycling temperatures, discharge and charge currents and depth-of-discharge.

The cycle life of a cell is defined in this paper as the number of charge/discharge cycles that the cell undergoes while maintaining its capacity above one half of its initial, or first cycle, capacity under the same cycling conditions. The capacity fade study determines the capacity after each cycle for a given charge and discharge condition at 37 °C. In our study, we are interested in obtaining an approximated cycle life for the particular type of cells, as oppose to an absolute number. Therefore, this information will provide us with a time frame within which the internal battery of the EVAD should be replaced. It should also be noted that the discharge current used in the cycle life study was the average current that the cells/battery would experience in the implanted EVAD device. The actual energy demanded by the device is of a pulsed nature, with a short high-current discharge pulse (typically 0.15–0.4 s at a 3–4 C rate, for a 'AA' size cell) followed by a low-current discharge (typically less than a C/2 rate, for a 'AA' size cell) for a period twice that of the high-current discharge duration. The effect of this type of discharge load profile on cycle life is currently under investigation in our laboratory.

Figure 7 shows the normalized discharge capacity plotted against the cycle number for the 'P' and 'H' type Ni/Cd cells and one 'S' type battery. Initially, the normalized capacities have a constant '100%' value since the discharge step was terminated at an 80% depth-of-discharge. However, the capacity eventually dropped below this specified depth-of-discharge after a number of cycles. At this point, the discharge step was then terminated at a voltage of 1.0 V for the cells and 10 V for the battery. The data from the 'S' type battery represents the average behaviour of ten cells. Cell voltage monitoring results showed very little difference in capacity among the cells of the battery. All three types of cells showed a similar slope to their capacity fade trends beyond their 65th cycle. However, there is a dramatic difference between the three types of cells before their 65th cycle, with the 'S' type cells showing a much higher capacity fade rate than the other two types of cells. It was also found that when an open-circuit period (typically longer than 24 h) was added after discharge, the cell capacity on the next discharge after the open-circuit period was higher than the preceding cycle. This higher capacity would soon drop to the original capacity fading trend on further cycling. This observed higher capacity, after the cell has been 'rested', may be the result of active electrode materials making recontact and/or remixing of the electrolyte.

Table 2 lists the extent of the capacity fade for each cell at its present cycle number. The 'S' type battery showed considerably less cycle life than the other two types of cells. This is not surprising as its performance is optimized for room temperature applications and not for higher temperatures. The cycle life of the 'P' and 'H' type cells could be considered to be similar, if we take into account the fact that the 'H' type cell was discharged at a slightly higher rate.

## Conclusion

Three types of Ni/Cd cells were studied at 37 °C in this preliminary evaluation. Their performance in terms of memory effect, discharge rate capability, self-discharge, surface temperature rise during charge and discharge and cycle life at the average EVAD operating current were evaluated and compared. Table 3 summarizes these characteristics for the three types of cells investigated. The performance of the 'P'

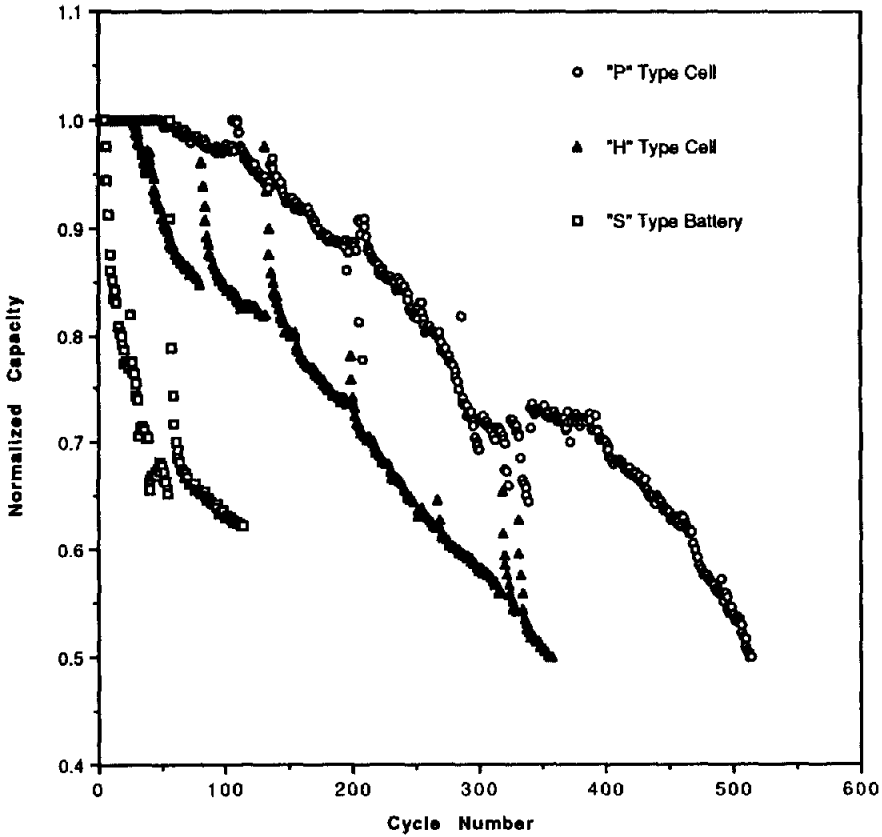


Fig. 7. Normalized capacity as a function of cycle number for the 'P' and 'H' type Ni/Cd cells and a 'S' type Ni/Cd battery at 37 °C.

TABLE 2

Capacity fade study of Ni/Cd cells/batteries cycled at 37 °C

Cell of battery type	Discharge rate (C)	No. of cycles	% of initial capacity remaining	Initial operating time (min)
'H' cell	1.50	358	50	28
'P' cell	1.35	514	50	32
'S' battery	1.46	114	62	29

and 'H' type cells are similar in terms of memory effect, cycle life and discharge rate capability. The 'S' type cells show a better high rate capability than the 'P' and 'H' type cells, although they suffer from memory effect and a shorter cycle life. The moderate discharge rate capability of 'P' and 'H' type cells may create some problems in the high power demanded of the EVAD. However, this problem may be solved by stringent quality control procedures ensuring that the selected cells for the internal

TABLE 3

Performance comparison of Ni/Cd cells tested at 37 °C

	'P' type	'S' type	'H' type
Memory effect	no	yes	no
Discharge rate capability	moderate	good	moderate
Self-discharge over 24 h	moderate	moderate	moderate
Surface temperature increase (charge)	safe	safe	safe
Surface temperature increase (discharge)	high	high	safe
Cycle life	medium	low	medium
Use in EVAD	possible	no	possible

battery are capable of high rate discharge. All three types of cells show comparable self-discharge rates. The surface temperature increases during discharge of the 'S' and 'P' type cells were very much higher than that for the 'H' type cell, which may damage surrounding tissue.

The 'S' type cells were rejected for the EVAD application due to, firstly, their short cycle life under EVAD operating conditions and, secondly, the existence of a memory effect and the possible energy management problems associated with it. The 'P' and 'H' type cells both show good performance characteristics and have potential for use as the internal power source for the EVAD. The use of the 'H' type cells is, however, slightly more desirable due to their lower surface temperature increase during discharge at EVAD conditions. The final choice of which cells would be best suited for the internal power source can only be decided after the safety and reliability of these cells have been determined.

### Acknowledgements

The authors wish to thank the Industrial Research Assistance Program (IRAP) of the National Research Council of Canada (NRCC), the Industrial Research Program of the Ontario Technology Fund (OTF) and Industry Science and Technology Canada (ISTC) for their financial support. They would also like to thank the other members of the EVAD Program team at the University of Ottawa Heart Institute, where this work was undertaken, for their helpful discussions and contribution to this work.

### References

- 1 R. K. Jarvik, *Sci. Am.*, 244 (Jan.) (1981) 74.
- 2 K. J. Korane, *Mach. Des.*, (Nov. 7) (1991) 100.
- 3 L. O'Connor, *Mech. Eng.*, (July) (1991) 36.
- 4 W. S. Pierce G. V. S. Parr, J. L. Myers, W. E. Pae, Jr., A. P. Bull and J. A. Waldhausen, *N. Engl. J. Med.*, 305 (1981) 1606.
- 5 D. G. Pennington, L. R. McBride, M. T. Swartz, K. R. Kanter, G. C. Kaiser, H. B. Barner, L. W. Miller, K. S. Naunheim, A. C. Fiore and V. L. Willman, *Ann. Thorac. Surg.*, 47 (1989) 130.

- 6 T. C. Mills, R. A. Ott and S. J. Barker, *Am. Soc. Artif. Intern. Organs Transpl. Abstr.*, 19 (1990) 59.
- 7 W. L. Holman, R. C. Bourge and J. K. Kirklin, *J. Thorac. Cardiovasc. Surg.*, 102 (1991) 932.
- 8 L. D. Joyce, K. E. Johnson, W. S. Pierce, W. C. DeVries, B. K. H. Semb, J. G. Copeland, B. P. Griffith, D. A. Cooley, O. H. Frazier, C. Cabrol, W. J. Keon, F. Unger, E. S. Bucherl and E. Wolner, *J. Heart Transplant.*, 5 (1986) 229.
- 9 P. M. Portner, P. E. Oyer, D. G. Pennington, W. A. Baumgartner, B. P. Griffith, W. R. Frist, D. J. Magilligan, Jr., G. P. Noon, N. Ramasamy, P. J. Miller and J. S. Jassawalla, *Ann. Thorac. Surg.*, 47 (1989) 142.
- 10 T. Mussivand, P. Diegel, J. Miller, G. K. MacLean, P. Santerre, R. G. Masters, P. J. Hendry, R. Robichaud, W. A. Adams, D. Olsen and W. J. Keon, *Proc. Cardiovasc. Sci. Techn. Conf., Bethesda, MD, Dec. 2-4, 1991*, p. 182.
- 11 G. D. Nagy, C. L. Gardner and W. A. Adams, *Transplant. Implant. Today*, (September) (1986) 56.
- 12 W. A. Adams, P. A. Aiken, C. M. Bank, G. K. MacLean and Z. Shu, *Proc. Electrochem. Soc. Conf., Fall Meet., Seattle, WA, Oct. 14-19, 1990*, p. 125.
- 13 W. A. Adams, P. A. Aiken, C. M. Blank, G. K. MacLean and Z. Shu, *Proc. Electrochem. Soc. Conf., Fall Meet., Seattle, WA, Oct. 14-19, 1990*, p. 126.
- 14 C. W. Sherman, F. L. Milder, T. C. Rintoul and D. H. La Forge, *Proc. 21st Intersoc. Energy Conversion Engineering Conf., San Diego, CA, Aug. 25-29, 1* (1986) 2132.
- 15 P. C. Milner and U. B. Thomas, in P. Delahay and C. W. Tobias (eds.), *Advances in Electrochemistry and Electrochemical Engineering*, Wiley-Interscience, New York, Vol. 5, 1967, p. 1.
- 16 E. J. Rubin and R. Baboian, *J. Electrochem. Soc.*, 118 (1970) 583.
- 17 M. Oshitani, M. Yamane and S. Hattorri, in J. Thompson (ed.), *Power Sources*, Vol. 8, Academic Press, New York/London, 1980, p. 471.
- 18 S. F. Pensabene and J. W. Gould II, *IEEE Spectrum*, (Sept.) (1976) 33.
- 19 T. R. Crompton, *Small Batteries, Secondary cells*, Vol. 1, Wiley-Interscience, New York, 1982.
- 20 R. Barnard, G. T. Crickmore, J. A. Lee and F. L. Tye, in D. H. Collins (ed.), *Power Sources*, Vol. 6, Academic Press, New York/London, 1976, p. 161.
- 21 A. J. Salkind and P. Bruins, *J. Electrochem. Soc.*, 109 (1962) 356.
- 22 W. H. Metzger, Jr., and J. M. Sherfey, *Electrochem. Tech.*, 2 (1964) 285.
- 23 J. C. Norman, G. LaFarge, R. Harvey, T. Robinson, L. Van Someren and W. F. Bernhard, *Am. Soc. Artif. Intern. Organs Transpl.*, 12 (1966) 282.
- 24 F. K. Storm, W. H. Harrison, R. S. Elliott and D. L. Morton, *Cancer Res.*, 39 (1979) 2245.
- 25 *Nickel/Cadmium Battery Application Handbook*, General Electric Company, Genium Publishing, Gainesville, FL, 3rd edn., 1986.
- 26 B. E. Conway and P. L. Bourgault, *Can. J. Chem.*, 37 (1959) 292.
- 27 P. C. Milner, *J. Electrochem. Soc.*, 107 (1960) 1.
- 28 E. J. Casey, A. R. Dubois, P. E. Lake and W. J. Moroz, *J. Electrochem. Soc.*, 112 (1965) 371.
- 29 S. U. Falk and A. J. Salkind, *Alkaline Storage Batteries*, Wiley-Interscience, New York, 1969.